



The Living Light Conference 2016

## Assessment of environmental spectral ellipsometry for characterising fluid-induced colour changes in natural photonic structures<sup>★</sup>

Mouchet S. R.<sup>a,b,\*</sup>, Van Hooijdonk E.<sup>b</sup>, Welch V. L.<sup>b</sup>, Louette P.<sup>b</sup>, Tabarrant T.<sup>b</sup>,  
Vukusic P.<sup>a</sup>, Lucas S.<sup>b</sup>, Colomer J.-F.<sup>b</sup>, Su B.-L.<sup>c,d</sup>, Deparis O.<sup>b</sup>

<sup>a</sup>School of Physics, University of Exeter, Stocker Road, Exeter EX4 4QL, United Kingdom

<sup>b</sup>Department of Physics, Physics of Matter and Radiation (PMR), University of Namur (UNamur), Rue de Bruxelles 61, B-5000 Namur, Belgium

<sup>c</sup>Laboratory of Inorganic Materials Chemistry (CMI), University of Namur (UNamur), Rue de Bruxelles 61, B-5000 Namur, Belgium

<sup>d</sup>Department of Chemistry and Clare Hall College, University of Cambridge, Herschel Road, Cambridge CB3 9AL, United Kingdom

---

### Abstract

Porous photonic structures found in several living organisms are known to display colour changes induced upon contact with liquids, vapours and gases. Usually these changes are due to physico-chemical phenomena such as the swelling of the structure enacted by the fluids, vapour physisorption on the pore walls, capillary condensation or a combination of them. Generally, the porous structures are open to outside, leading to fast fluid exchanges with the surrounding environment and consequently fast colour changes. In this article, we first introduce fluid-induced optical changes in living organisms exhibiting porous photonic structures. We explore then the potentiality of environmental ellipsometry for the first time in the context of natural photonic structures through the investigation of the optical response of the male cerulean chafer beetle *Hoplia coerulea* (Scarabaeidae) upon contact with water, 2-propanol and toluene vapours. In contrast with most of the investigated photonic structures, this beetle's structure is encased by an envelope that mediates liquid exchanges with the environment. Such a study is of great interest in order to understand the underlying biological functions behind these changes as well as in order to develop bioinspired applications such as gas sensors and other environment-responsive coatings.

© 2017 Elsevier Ltd. All rights reserved.

Selection and Peer-review under responsibility of The Living Light Conference (May 4 – 6) 2016, San Diego (USA).

**Keywords:** Structural colours; photonic crystals; optical sensors; photonic bandgap materials; natural photonic crystal; colour; ellipsometry

---

<sup>★</sup> This is an open-access article distributed under the terms of the Creative Commons Attribution-NonCommercial-ShareAlike License, which permits non-commercial use, distribution, and reproduction in any medium, provided the original author and source are credited.

\* Corresponding author. Tel.: +44 (0)1392 724156.

E-mail address: [s.mouchet@exeter.ac.uk](mailto:s.mouchet@exeter.ac.uk)

## 1. Introduction

The colourations of several living organisms such as chameleons [1], various families of arthropods (Chrysomelidae, Libellulidae, Papilionidae, Pentatomidae, Scarabaeidae, etc.) [2,3], of fish (e.g., Nemipteridae) [4] and of birds (Columbidae, Hirundinidae, etc.) [5,6] are known to change dynamically and reversibly (Fig. 1). For instance, a recent review regarding only such changes in arthropods listed more than 120 species displaying colour changes following different environmental and endogenous stimuli [3]: grasshoppers, damselflies, spiders, beetles or stick insects, among others. These changes can be very fast and occur with pigmentary colours (i.e., colourations due to pigments) and structural colours (i.e., colourations due to coherent scattering in photonic structures). They are divided into active and passive colour changes. The former changes are controlled by the living organisms' metabolisms through their nervous or endocrine systems [1,4,7] in response to the background colouration (for camouflage), temperature changes or the animal's excitation or reproduction state. The latter are induced by the surrounding environment [5,6,8-10] through a modification of the atmosphere composition (change in the relative humidity) or contact with liquids.

The biological functions (e.g., thermoregulation, protection against UV, camouflage, aposematism, intraspecific signalling, etc.) behind such changes often turn out to be more obvious in the case of active changes than with passive changes which sometimes may constitute a fortuitous consequence of other organisms' functions. However, these changes and particularly fluid-induced colour changes in porous photonic structure offer new possibilities to design photonic materials inspired by these natural mechanisms such as vapour and gas-sensors [11-16].

In this article, we first introduce fluid-induced colour changes in living organisms displaying photonic structures and some bioinspired applications with a brief review of the literature. We assess then the changes of optical reflection from elytra of the male cerulean chafer beetle *Hoplia coerulea* (Scarabaeidae) in contact with vapour of water, 2-propanol and toluene using environmental ellipsometry [17] from both experimental and numerical approaches.

## 2. Brief review of fluid-induced colour changes in natural photonic structures

Already in the 1920s Mason highlighted colour changes in iridescent bird feathers and insect wings upon contact with liquids characterised by a refractive index different from the feather and wing materials [18-21]. However, the most well-known example of fluid-induced colour changes is the case of *Morpho* butterflies, the wings of which turn from a metallic blue colouration to a metallic green colouration when a droplet of alcohol is deposited on them [22-24]. The photonic structures of these insects are located on the scales covering their wings. They comprise parallel ridges composed of stacks of lamellae spaced by air gaps [25,26]. The cross sections of these structures are known to resemble a Christmas tree. Following the deposition of alcohol droplets, the liquid fills the air gaps, leading to modifications of the optical properties of the photonic structures and consequently of the butterfly's colouration. Such a simple experiment is often performed in order to distinguish structural colours from pigmentary colours. Furthermore, impregnation of natural photonic structures with a refractive index matching liquid is often used in order to remove the optical effects of structures such as light reflection. This enables, for instance, the investigation of absorption by pigments embedded in these structures [18-21,25,27,28]. A recent study [24] compared the liquid-induced colour changes of the scales of the Rhetenor Blue *Morpho* butterfly *Morpho rhetenor* (Nymphalidae) (exhibiting a Christmas tree structure) and the Green Swallowtail butterfly *Papilio blumei* (Papilionidae) (displaying a concave porous multilayer) and showed that the variations of reflectance intensity and shift of the peak position were more striking with the latter because of the larger porous volume of *P. blumei*'s photonic structure.

The colour changes induced by filling of porous photonic structure were also observed in beetles' photonic structures. The greenish colour of the male Hercules beetle *Dynastes hercules* (Scarabaeidae) (one of the biggest beetle worldwide) is due to coherent scattering and light diffraction in a porous structure located in the insect's cuticle under a 3  $\mu\text{m}$ -thick homogeneous layer [8,29]. Modelled by a three-dimensional photonic crystal, this structure comprises columns made of cuticle material, perpendicular to the elytra surface and connected by chitinous filaments. Upon contact with water or an atmosphere with a relative humidity higher than 80%, water penetrates into the structure through cracks in the external layer. The photonic structure reversibly becomes almost transparent

through the homogenisation of the refractive index and the colouration of the beetle's elytra turns to black due to the presence of an underlying absorbing layer composed of melanin [8,29].

The tortoise beetle *Charidotella egregia* (Chrysomelidae) is able to modify reversibly and actively its colouration following a tactile stimulus within a few tens of seconds [7]. The golden colour of the head, the prothorax and the elytra of this coleopteran is due to a chirped multilayer reflector located in the exocuticle and turns to transparency after a stimulus. In this case, the underlying layer is a pigmentary diffuse red layer. This colour change was explained by the draining of the physiological liquid, most likely hemolymph, located in the multilayer leading to the loss of the reflector's coherence and to its transparency.

Generally, photonic structures in insects are open to the surrounding environment and the fluid enacting colour changes. This feature gives rise to fast fluid exchanges since they can easily penetrate into the structure. The related colour changes are consequently fast. However, photonic structures which are not open such as beetle scales can also exhibit fluid-induced colour changes. In the case of the male cerulean chafer beetle *H. coerulea* (Fig. 1a) [30,31], the blue-violet scales covering its elytra and thorax are known to change to green colour upon contact with liquids (Fig. 1b) [10,32–34]. The structure is a porous periodic multilayer comprising dense planar layers and porous spacer layers encased by an envelope that separates the structure from the environment (Fig. 1c) [10,31]. The colour change was explained by the filling of the structure's pores following liquid infiltration through the permeable envelope [10,34]. The encasing envelope was shown to mediate the liquid exchange and to control the colour change, depending on the tested liquid. Because of the mediating role of this envelope, the system comprising the photonic structure and the envelope was called "photonic cell" [34].

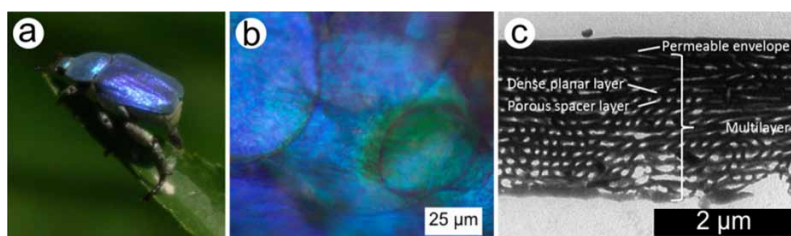


Fig. 1. The male cerulean chafer beetle *H. coerulea* (Scarabaeidae) displays a blue-violet iridescent colour (a) due to scales covering its thorax and elytra (b). Inside the scales, a porous multilayer photonic structure is encased by a permeable envelope (c). Upon contact with water (here a nanoliter droplet was deposited on a scale), the blue-violet coloration turns to green (b).

A similar multilayer structure is found inside the flat and long scales covering the elytra of the beetle *Tmesisternus isabellae* (Cerambycidae) [9]. These scales display a golden iridescent colour which turns to red upon contact with water. This colour change was shown to be a result of another phenomenon involved in passive colour changes, in addition to the filling of the air pores: the swelling of the dense planar layers [9]. Because of the infiltration of water molecules, hydrogen bonds between biopolymer molecules disrupt leading to a swelling of the structure and hence the increase of the structure's period.

In a similar way to the effect described for *T. isabellae* beetle, the swelling of the photonic structure due to contact with water and relative humidity variations was also observed in some bird feathers. The phenomenon led to fast and reversible colour changes. The iridescent colourations of bird feathers are generally due to thin film interference in one single keratin layer comprising the external cortex of the feather barbules [5,6]. In the case of the violet-pink feathers of the mourning dove *Zenaidra macroura* (Columbidae), in addition to the swelling of the structure upon contact with water, the barbules rotate at their attachment points with respect to the feather barbs due to mechanical constraints, leading to an increase of the surface illuminated by incident light [6]. The blue-green feathers of the tree swallow *Tachycineta bicolor* (Hirundinidae) turn to yellow-green when the relative humidity increases and enacts the swelling of the keratin layers [5]. Upon drying, the material shrinks and the feathers exhibit their original colouration.

Besides direct contact with liquids, variations in the surrounding atmosphere composition can also give rise to colour changes in insects' photonic structures. In 2007, Potyrailo *et al.* highlighted changes in the optical response of the *Morpho sulkowskyi*'s wings [35] induced by vapours of water, methanol, ethanol and isomers of dichloroethylene. The measured reflectance variations were so specific to the tested vapours that they could be

individually identified based on their responses. It is interesting to note that despite the hydrophobicity of *Morpho*'s wings [26], water vapour penetrates the structure's pores and adsorbs on their walls. In addition to the high selectivity, the optical response was also shown to be very sensitive to low concentrations: the smallest reported detected concentration ranged from 1 to 2 p.p.m. In spite of the fact that water, methanol and ethanol have similar polarities and refractive indices, the differences in the reflected optical response allowed to discriminate between these three fluids, at relative pressures as low as 2%. Furthermore, three isomers of dichloroethylene (1,1-DCE, trans-1,2-DCE and cis-1,2-DCE) which are closely related could be differentiated. Such fluid-induced colour changes were also highlighted a few years later in the case of *Morpho didius* [22,36,37]. Later on, the same researchers explained the origin of these colour change selectivity by a polarity gradient along the vertical axis of the ridges. The latter are more polar at the top [38]. Depending on its polarity, vapour adsorbs preferentially at the top or the bottom of the ridges.

In 2008, Biró et al. [39] investigated 20 butterfly and moth species displaying optical response to six vapours (water, ethanol, acetone, chloroform, pentane and benzene) and one gas (ammonia) that was selective, sensitive, reproducible and fast. Among these butterflies and moths, *Chrysidia rhipheus* (Uraniidae), *Pseudolycaena marsyas* (Lycaenidae), the ventral wings of *Cyanophrys remus* (Lycaenidae) and *Morpho aega* (Nymphalidae) exhibited very different photonic structures: porous multilayers, photonic polycrystals and Christmas tree structures. All of them gave rise to detectable colour changes induced by the seven tested vapours. Their optical responses also depended on the concentration. In the cases of *Polyommatus icarus* (Lycaenidae), *Polyommatus bellargus* (Lycaenidae) and *Polyommatus coridon* (Lycaenidae), spectral variations were found to be linear with respect to the concentration [40]. If human eyes are not able to distinguish colour changes (peak wavelength shift less than 10 nm) induced by low concentrations (less than 50%) of vapours of acetone, acetic acid, ethanol, 2-propanol, chloroform, toluene and water, butterflies' eyes would be able to, in the case of *P. icarus*, according to researchers of the same group [41]. However, the biological role of these changes is still unknown. Moreover, it is likely that these butterflies are regularly in contact only with water vapour among the tested ones. Following the deposition of 5 nm-thick layer of Al<sub>2</sub>O<sub>3</sub>, the sensibility and selectivity of *P. icarus*' wings were found to be reduced, indicating clearly that other factors (probably related to the surface chemistry of the material) than the structure geometry and the refractive indices influence the vapour-induced colour changes of these butterflies [41].

Temperature-induced colour changes were reported in the cases of these three *Polyommatus* butterfly species [40,42] as well as with *M. aega* [42,43], *Callophrys rubi* (Lycaenidae) and *C. remus* [43] between -10°C and ambient temperature. Upon contact with a vapour at lower temperature, colour changes were found to be more significant than at ambient temperature [40,42]. The origin of these colour changes induced by vapours and temperature would be capillary condensation of vapour within the structures' pores according to the pore sizes, leading to changes in the refractive index contrast between the structure material and the pore content [40-43]. At higher concentrations (more than 50%), a swelling of the structure would occur and play a dominant role in the colour changes [41].

### 3. Bioinspired applications

Following these investigations, several research groups started to develop gas and vapour sensors inspired by these living organisms. The purpose is to design such sensors through replication, mimicking and optimisation of the structure geometries and material compositions from the point of view of their response to fluids [13] or even use directly organisms' photonic structures bred for that purpose, after possible modifications [41,44]. These sensors are of great interest from a technological point of view in various fields such as perfume industry, food industry, wood industry, air pollution and air quality management, explosive and narcotic detection, breath alcohol measurement, medical diagnosis and gas storage.

These sensors have to be able to distinguish between different kinds of gases as well as to give an indication regarding the concentrations within a short response time. A quantitative measurement of these concentrations can be performed through image processing or spectrophotometry. One claimed advantage of such optical sensors is to be based on human vision, one of the human most efficient senses, in order to detect variations that are not easily perceived by human sense of smell. Furthermore, this sensing based on optical signal detection without electronic system and power supply could be advantageous in flammable and explosive atmospheres. Due to the reversibility of

the colour changes, such bioinspired sensors will not need regeneration by heating. Finally, the optical properties of natural photonic structures are robust against production defects: they are not much affected by them [45]. This constitutes an obvious advantage from an industrial point of view. One main drawback is that such sensors can be damaged by some vapours and gases. Furthermore, due to their sensitivity to temperature, it is important to control or take temperature variations into account in order to obtain accurate measurements.

The photonic structure of *Morpho* butterflies has inspired gas sensor designs. Potyrailo *et al.* recently synthesised a very accurate analogous structure, from the physical and chemical points of view, that selectively detects and quantifies vapours (benzene, methyl ethyl ketone, acetonitrile, methanol and water) in mixtures [15]. The structure was fabricated using electron beam lithography, by patterning a periodic stack comprising 100-nm thick layers of poly(methyl methacrylate) (PMMA) and a copolymer of methyl methacrylate (MMA) and methacrylic acid (MAA). The Christmas tree structure was functionalised through a spatially controlled coating with monolayers of fluorine-terminated silane and an amine-terminated silane. Vapour sensors mimicking the architecture of *Morpho* butterfly scales were also fabricated by Atomic Layer Deposition (ALD) of  $\text{Al}_2\text{O}_3$  and  $\text{TiO}_2$  layers as well as of  $\text{Al}_2\text{O}_3$  and  $\text{HfO}_2$  layers [16]. These results showed that the optical response of the mimicked structure was selective to ethanol and 2-propanol vapours.

A humidity sensor was inspired by the *D. hercules* structure [11]. The sensor was a three-dimensional porous photonic structure made of poly(ethylene glycol)-diacrylate (PEG-DA). Its colour changes, from blue-green in the dry state to red in higher relative humidity, are due to the filling of the pores and the swelling of the polymer. Other humidity sensors based on periodic organic/inorganic hybrid multilayers similar to those found in the paradise whiptail *Pentapodus paradiseus* (Nemipteridae) were also synthesised [46]. This fish displays blue stripes on its body and head [4]. The colouration of these stripes is due to iridophores and can change to red after the release of hormones. The bioinspired multilayers were made of  $\text{TiO}_2$  layers and poly(2-hydroxyethyl methacrylate-co-glycidyl methacrylate) (PHEMA-co-PGMA) layers. Although the colour changes of the fish is not induced upon contact with liquids or vapour, the polymer layers of the sensor swell after exposure to water vapour, leading to colour change.

The multilayer structure of *T. isabellae* inspired mesoporous colloidal photonic crystals that were sensitive to vapours [47]. These photonic crystals were synthesised by inkjet printing of silica ( $\text{SiO}_2$ ) nanoparticles that spontaneously assemble during ink drying. Changes in the reflected intensity are enacted by water vapour condensation in the interstitial spaces. The optical response was shown to be linear with respect to relative humidity. Similarly, silk-fibroin inverse opals inspired by this longhorn were designed [48]. In this case, the swelling enacted by water, leads to changes in the structure dimensions, in addition to pore filling that changes the refractive index contrast.

Environment-responsive glass windows were also developed based on these natural phenomena. The change from structural colour to transparency observed in *C. egregia* inspired coatings made of mesoporous  $\text{TiO}_2$  and  $\text{SiO}_2$  multilayers that reversibly display a structural colour after infiltration by liquids [12,14].

Many optical gas sensing devices are currently developed, based on various technologies. See review papers [49,50]. The optical systems implemented through nanotechnologies rely on phenomena such as localised plasmon resonances, Bragg diffraction or Fabry-Pérot interference. Bioinspired optical sensors are hence in competition with them. The main challenge, during the design of a gas sensor is, depending on the application, to distinguish the largest number of volatile components (i.e., high selectivity) in addition to reaching the best resolution, the highest sensitivity, the shortest response time, the largest measurement dynamics, a long term stability, the smallest size, the lowest energy consumption, an ease of maintenance, the lowest production or running costs. The idea is to find the sensing applications for which bioinspired photonic structures can provide with a better trade-off between the requirements than other kinds of gas sensors. One of the sensing applications that is sometimes claimed is portable gas sensors for which bioinspired optical structures could lead to increased selectivity and resolution with respect to existing sensors.

#### 4. Environmental spectral ellipsometry as analysis tool

When light reflects on an optical sample, its polarisation state changes. This change is related to the sample's optical properties (i.e., refractive indices) and geometry (e.g., layer thicknesses). Ellipsometry quantifies these

changes in polarisation states through ellipsometric parameters  $\cos \Delta$  and  $\tan \Psi$  (Fig. 2a). These two parameters are linked by the fundamental equation of ellipsometry:

$$\rho = \frac{r_p}{r_s} = \tan \Psi e^{i\Delta} \quad (1)$$

where  $\rho$  depends on the refractive indices of the investigated sample's materials, its geometry, the incidence angle and the wavelength;  $r_p$  and  $r_s$  are Fresnel coefficients for the p- and the s-polarisations, respectively;  $\tan \Psi = |r_p/r_s|$  is the module of the ratio;  $\Delta = \delta_p - \delta_s$  is the phase change difference between both polarisations. Fresnel coefficients  $r_p$  and  $r_s$  represent electric field intensity and phase modifications after reflection on the sample:

$$r_j = \frac{E_{jr}}{E_{ji}} = |r_j| e^{i\delta_j} \quad (2)$$

where  $j$  stands for the polarisation (p and s);  $E_{jr}$  and  $E_{ji}$  are the corresponding intensities of the electric fields  $\vec{E}_r$  (reflected) and  $\vec{E}_i$  (incident), respectively;  $\delta_j$  is the phase change induced by the reflection.

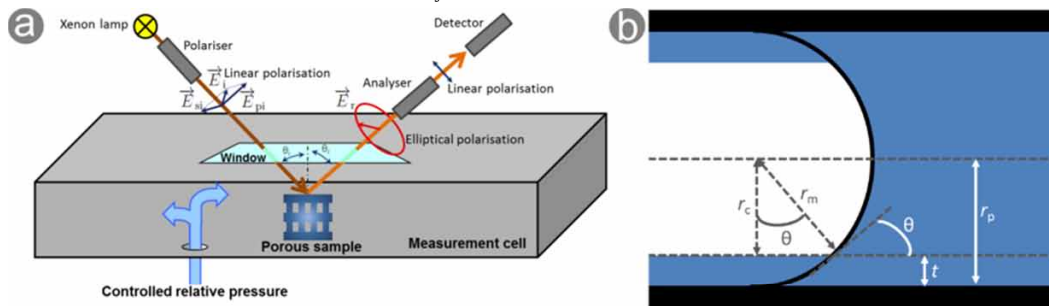


Fig. 2. a) In ellipsometry, a polariser is inserted in the incident beam path. An analyser and a detector allow to measure changes in polarisation state after reflection on the sample. When equipped with a hermitical measurement cell in which the atmosphere composition is controlled, environmental ellipsometry measurements can be performed. b) Cross section parallel to the axis of a cylindrical pore characterised by a radius  $r_p$  in which a physisorbed film with a thickness  $t$  and a hemispherical meniscus with a radius of curvature  $r_m$  formed. The relation between the core radius  $r_c$  of the pore and  $r_m$  is  $r_c = r_m \cos \theta + t$  with the contact angle  $\theta$ .

Ellipsometric parameters  $\cos \Delta$  and  $\tan \Psi$  hence contain more physical information than reflectance measurements since they convey information about the phase of the reflected light and not only about the intensity.

Several ellipsometric techniques exist. All of them are based on the same principle (Fig. 2a) [51]: one polariser is inserted in the incident beam path in order to select its polarisation state. An analyser and a detector are used to measure polarisation changes due to reflection. One of the most common techniques uses a rotating polariser: the incident beam is polarisation-modulated through the rotation of a polariser. Before reflection on the studied sample, incident light polarisation is linear whereas the reflected light is elliptically polarised.

By approximating the investigated sample by a stratified optical model, these measurements allow to retrieve the (effective) refractive indices of the different layers and of the substrate, as well as the layer thicknesses [51]. To that end, numerical spectra computed with adjustable layer thicknesses and (complex) refractive indices of the model are fitted to experimental spectra. A structure model made of  $N$  layers leads to  $3N + 2$  fitting parameters (real and imaginary parts of the refractive indices of the layers and the substrate as well as the layer thicknesses).

Ellipsometry is a technique that is very sensitive to the sample's surface properties and is more stringent than reflectometry because it requires a very accurate model of the sample for fitting experimental data. Because of the modelling of the sample's structure, ellipsometry requires flat sample surface. Sub-wavelength roughness can be however tolerated by modelling it as an effective medium surface layer.

When equipped with a cell controlling the surrounding atmosphere [17] (Fig. 2a), measurements of the dynamics in  $\cos\Delta$  and  $\tan\Psi$  induced by vapour in porous samples may enable to quantify changes in refractive indices and thicknesses through vapour adsorption and desorption in the sample's pores allowing to bring valuable information regarding the mechanical (e.g., Young's modulus) and porosity (porous volume, pore sizes, etc.) properties [12]. This technique is called ellipsoporosimetry and is even more stringent than ellipsometry.

Porosity influences indeed vapour adsorption and desorption. At low relative pressure  $P/P_s$  (vapour partial pressure:  $P$ , saturation vapour pressure:  $P_s$ ), a liquid film adsorbs on the walls of mesopores (i.e., pores with a size ranging from 2 nm to 50 nm) and macropores (i.e., pores, the size of which is larger than 50 nm). At higher relative pressure, depending on the shape and size of pores, the adsorbed film may form a meniscus (i.e., a curved liquid surface in the neighbourhood of a solid surface) and capillary condensation may occur, i.e., vapour instantaneously condenses and fills up mesopores, the critical sizes of which depend on the relative pressure. The relation between the relative pressure  $P/P_s$  giving rise to capillary condensation and the radius of curvature  $r_m$  of a hemispherical meniscus is given by the Kelvin equation [52,53]:

$$\ln\left(\frac{P}{P_s}\right) = -\frac{2\gamma_{LA}V_L}{RT r_m} \quad (3)$$

where parameters are the liquid-air surface tension  $\gamma_{LA}$ , the liquid molar volume  $V_L$ , the ideal gas constant  $R = 8.31447 \text{ J/K mol}$  and the absolute temperature  $T$ . The radius of curvature  $r_m$  hence depends on the adsorbate and the temperature. Kadlec and Dubinin [54] showed that capillary condensation occurs with a minimal radius of curvature  $r_{m,\min}$  equal to  $11.0 \text{ \AA}$  at  $T = 20^\circ\text{C}$  with water. This value corresponds to a relative pressure

$$P/P_s = \exp\left\{-\left(\frac{2\gamma_{LA}V_L}{RT r_m}\right)\right\} = 0.375 \text{ with } \gamma_{LA} = 0.07275 \text{ N/m and } V_L = 1.805 \times 10^{-5} \text{ m}^3/\text{mol}.$$

This means that below a relative humidity equal to 37.5%, capillary condensation cannot occur with water vapour at  $20^\circ\text{C}$  regardless of the pore size. Given this relative pressure, the adsorbed film thickness  $t$  before capillary condensation occurs is equal to 4.4 nm [53,55]. In such a case, the pore radius  $r_p$  is equal to  $r_p = r_c + t = r_{m,\min} \cos\theta + t = 5.4 \text{ nm}$  where the core radius of the pore is  $r_c$  and the contact angle  $\theta$  of a water droplet on elytra of the male beetle *H. coerulea* is equal to  $76^\circ$  [34] (Fig. 2b). Pores smaller than 5.4 nm will be directly filled at lower water vapour partial pressure with a few water molecules, without physisorption of a liquid film giving rise to a meniscus.

Most of the investigated natural photonic structures displaying colour changes induced by water vapour are characterised by pores, the sizes of which range from approximately 50 nm to a few hundreds of nanometres. Using similar calculation, it can be shown that in pores with a radius  $r_p = 50 \text{ nm}$ , capillary condensation occurs with a relative humidity equal to 97.7% after the adsorption of 11.2 nm-thick film, in the case of a hemispherical meniscus. Capillary condensation with such a pore size cannot therefore be at the origin of the observed colour changes at ambient temperature, specifically at lower partial pressures. Physisorption of vapour on pore walls can lead to noticeable colour changes [56]. Another explanation could be capillary condensation and pore filling in much smaller pores (and hence at much lower partial pressure) which would be present in the investigated photonic structures and give rise to the increase of the effective refractive index but would not be at the origin of coherent scattering since they would not interact with visible light because of their small sizes.

## 5. Assessment via experiment of environmental ellipsometry for characterising vapour-induced changes in a beetle elytron

In all the examples of vapour-induced colour changes reviewed here above, the photonic structure is open to the surrounding environment. However, changes in non-open photonic structures were observed in the case of *H. coerulea* (Fig. 1) [57]. Its response to vapour exposure was marked by a redshift of the reflectance peak and an

increase in peak reflectance intensity. The latter feature is not usually associated with fluid-induced reflectance changes. Simulations showed that this arises from the adsorption of a film on the scales' surface followed by the penetration of the liquid through the scales' envelope and the filling of micropores in the scales material [57].

Because of the fact that the reflectance changes induced by vapour are well-known in that beetle species, we used its elytra in order to assess, for the first time in the context of natural photonic structures, environmental spectral ellipsometry [17] as an analysis tool for characterising the vapour-induced changes of the optical properties of beetle elytra. We analysed the changes of these optical properties through the measurement of ellipsometric parameters  $\cos\Delta$  and  $\tan\Psi$  (as a function of incident wavelength) upon contact with vapours of water, 2-propanol and toluene (with relative pressures ranging from 0% to 100%).

Natural photonic structures are a priori very challenging to analyse with ellipsometry because of their roughness and disorder, preventing an accurate sample modelling. Usually, such a model is accurate enough for reflectance spectra but this is not the case with  $\cos\Delta$  and  $\tan\Psi$  spectra. Our aim is to assess the capacity of environmental spectral ellipsometry for highlighting vapour-induced optical changes, taking into account the fact that the above discussed stringent requirements on the sample are a priori not fulfilled: the sample surface is smooth but curved, spoiling detection of specularly reflected light and the sample's structure is complex, preventing attempt of data fitting because of the high number of model parameters.

Our measurements were performed with a Semilab Sopra EP series GES5 ellipsometer equipped with a 75 W xenon lamp. The spot size of the incident beam was about  $1\text{ mm}^2$ . The incidence and detection angles were equal to  $60^\circ$  with respect to the normal to the samples. The time-lapse between two consecutive measurements at two different relative pressures was chosen to be equal to 15 s in order to highlight the fastest features of the optical changes.

In spite of the challenging conditions of these measurements, reproducible changes in ellipsometric parameters  $\cos\Delta$  and  $\tan\Psi$  are observed. Upon contact with water and toluene vapours,  $\cos\Delta$  and  $\tan\Psi$  spectra are reversibly redshifted by about 10 nm and 4 nm, respectively (Fig. 3). In the case of 2-propanol, the spectra are not significantly modified (Fig. 3c-d). This difference in sensitivity is in agreement with previous studies regarding liquid- and vapour-induced reflectance changes [34,57]: water enacts more significant changes in *H. coerulea*'s response than toluene and quite more significant changes than 2-propanol.

## 6. Assessment via modelling of environmental ellipsometry for characterising vapour-induced changes in a beetle elytron

Simulations involving different physico-chemical processes at the origin of the measured optical responses were performed. As mentioned above, it is illusory to establish a model that will reproduce perfectly the experimentally observed changes. The aim here is to give possible explanations for these changes.

Simulations of the  $\cos\Delta$  and  $\tan\Psi$  spectra were performed using a custom-built thin-film modelling computer code relying on 1D scattering matrix formalism [58] for the beetle scales' photonic structure modelled as a periodic stack of 12 bilayers comprising 160 nm-thick dense planar layers and 35 nm-thick spacer layers. The incidence angle was taken equal to  $60^\circ$ , as in experiment. The refractive indices of the cuticle material and air were  $n_{\text{cuticle,eff}} = 1.56$  [59] and  $n_{\text{air}} = 1.00$ , respectively (Fig. 4). The agreement with the experimental spectra is not good, as expected. However the main features of the measured spectra (e.g., minima around 400 nm in  $\cos\Delta$  spectra and maxima around 400 nm in  $\tan\Psi$  spectra, framed in orange in Fig. 3) are present in the simulations. Fits of the measured spectra with respect to the layer thicknesses and refractive indices are not accurate enough in order to deduce quantitative results from this ellipsometric investigation (such as pore sizes). The natural samples we used in our measurements are far from being well ordered photonic structures: they are not flat, and display a lot of defects (e.g., roughness and disorder) in their many different layers presenting different porosities. Ellipsometric parameters are very sensitive to such defects, at the contrary of reflectance. Furthermore, experimental incidence and detection angles are not very well defined because of the scales orientations on the elytra. Notably, measurements on beetle elytra performed using Mueller-matrix ellipsometry are known to allow fitting of the 16 ellipsometric elements of the measured Mueller matrices [60-62]. In these cases, the photonic structures are located in the exocuticle of the beetles' elytra and not in scales covering the elytra.

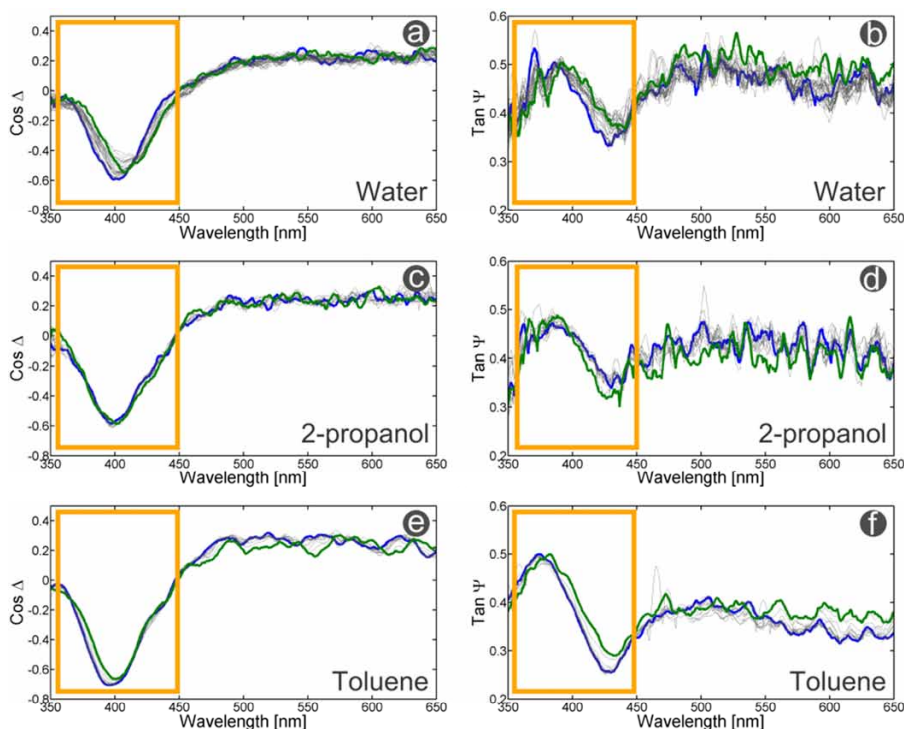


Fig. 3. Spectra of ellipsometric parameters ( $\text{cos}\Delta$  and  $\text{tan}\Psi$ ) measured with a  $60^\circ$ -incidence angle on an elytron of the male *H. coerulea* beetle upon contact with vapours of water (a-b), 2-propanol (c-d) and toluene (e-f). Relative pressures increase from 0% (blue curves) to 100% (green curves). Grey curves correspond to intermediate relative pressures. Reversible changes are observed with relative pressures decreasing from 100% to 0%. The main features that are similar to the simulated spectra are framed in orange.

Because of the fact that the *H. coerulea*'s photonic structure is not open to the surrounding environment, its colour changes cannot be explained by physisorption of vapour on the pore walls or capillary condensation within the pores. As we showed in a previous article [57], the likeliest process at the origin of these changes is the physisorption of a thin film on the scales' surface followed by penetration of liquid through the photonic structure micropores, leading to the increase of the refractive index  $n_{\text{cuticle,eff}}$  of the cuticle material.

If these two effects are assumed, a shift of the simulated  $\text{cos}\Delta$  and  $\text{tan}\Psi$  spectra is also predicted (Fig. 4), in accordance with the experimental results. In these simulations, the film thickness and the liquid penetration into the scale material are parameters which depend on partial pressure.

## 7. Conclusion

Structural colourations of insect wings can be modified upon contact with liquids and vapours. The majority of the photonics structures giving rise to such changes that have been investigated so far are porous and open to the surrounding environment. Through experimental and numerical approaches, we explored the potentiality of environmental ellipsometry as a new characterisation tool in the context of natural photonic structures. For that purpose, we investigated the particular case of the male *H. coerulea* beetle which displays liquid- and vapour-induced colour changes despite the fact that its porous photonic structure is not open to the environment but encased by an envelope that separates the structure and external fluids. In spite of the stringent requirements imposed by this technique on the sample, reproducible changes in ellipsometric parameters  $\text{cos}\Delta$  and  $\text{tan}\Psi$  of light reflected by its elytra upon contact with water, 2-propanol and toluene vapours were measured. Similarly to liquid-induced colour changes, these measurements showed that this beetle's scales are more sensitive to water than to alcohol. These changes were further explained by simulations of the variations due to the adsorption of a liquid thin film on the scales' surface and the filling of the structure material's micropores leading to the increase of the refractive index.

Investigating these fluid-induced optical changes is of great interest in order to understand the underlying biological functions behind these effects as well as in order to develop applications in fields such as gas and vapour sensing, environment-responsive glass windows, medical diagnosis and cell-metabolism monitoring through a bioinspired approach.

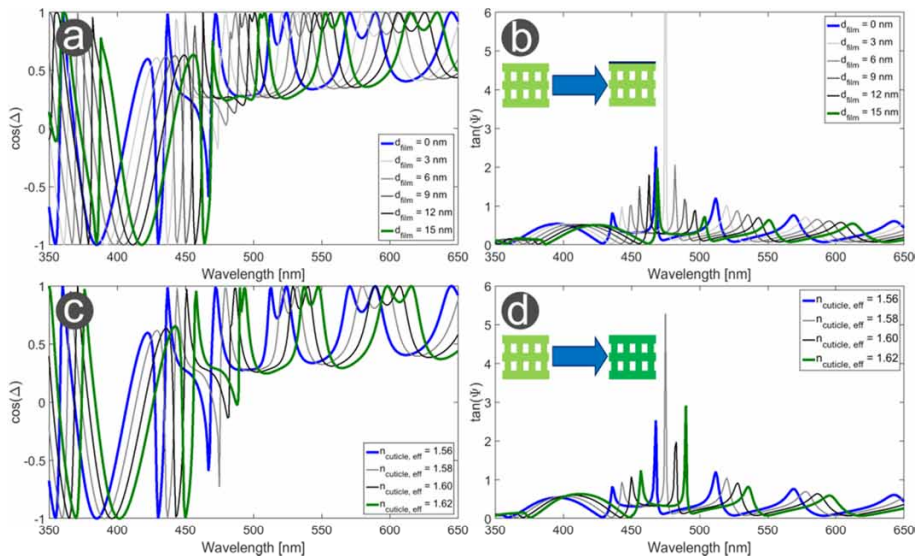


Fig. 4. Simulated spectra of ellipsometric parameters ( $\cos\Delta$  and  $\tan\Psi$ ) with a  $60^\circ$ -incidence angle on the *H. coerulea*'s modelled photonic structure comprising cuticle material ( $n_{\text{cuticle,eff}} = 1.56$ ) [59] and air ( $n_{\text{air}} = 1.00$ ), (a-b) onto which a liquid film is adsorbed (thickness  $d_{\text{film}}$  ranging from 0 nm to 15 nm and  $n_{\text{film}}$  equal to 1.33) and (c-d) when the refractive index  $n_{\text{cuticle,eff}}$  of the cuticle material increases from 1.56 to 1.62 due to infiltration of liquid in the material micropores.

## Acknowledgements

The authors thank Louis Dellieu (Department of Physics, UNamur) for technical support during the collection of samples. S.R.M. was supported by the Belgian National Fund for Scientific Research (F.R.S.-FNRS) as a Research Fellow, by Wallonia-Brussels International (WBI) through a Postdoctoral Fellowship for Excellence program WBI.WORLD and by the Royal Academy of Science, Letters and Fine Arts of Belgium through a grant of the Agathon De Potter Fund. E.V.H. and J.-F.C. were supported by F.R.S.-FNRS as Postdoctoral Researcher and Research Associate, respectively. This research was also supported by F.R.S.-FNRS through the Research credit CDR J.0035.13. It used resources of the "Plateforme Technologique de Calcul Intensif (PTCI)", UNamur (<http://www.ptci.unamur.be>), which is supported by F.R.S.-FNRS under convention No. 2.4520.11 as well as of the Electron Microscopy Service (SME), UNamur (<http://www.unamur.be/en/sevmel>). PTCI and SME are members of the "Consortium des Équipements de Calcul Intensif (CÉCI)" (<http://www.ceci-hpc.be>) and of the "Plateforme Technologique Morphologie – Imagerie" (UNamur), respectively.

## References

- [1] J. Teyssier, S.V. Saenko, D. van der Marel, M.C. Milinkovitch, Nat. Comm. 6 (2015) 6368.
- [2] R. Silberglied, A. Aiello, Science 207 (1980) 773-775.
- [3] K.D.L. Umbers, S.A. Fabricant, F.M. Gawryszewski, A.E. Seago, M.E. Herberstein, Biol. Rev. 89 (2014) 820-848.
- [4] L.M. Mähger, M.F. Land, U.E. Siebeck, N.J. Marshall, J. Exp. Biol. 206 (2003) 3607-3613.
- [5] C.M. Eliason, M.D. Shawkey, Opt. Express 18 (2010) 21284-21292.
- [6] M.D. Shawkey, L. D'Alba, J. Wozny, C. Eliason, J.A.H. Koop, L. Jia, Zoology 114 (2011) 59-68.
- [7] J.-P. Vigneron, J.M. Pasteels, D.M. Windsor, Z. Vértesy, M. Rassart, T. Seldrum, J. Dumont, O. Deparis, V. Lousse, L.P. Biró, D. Ertz, V.L. Welch, Phys. Rev. E 76 (2007) 031907.
- [8] M. Rassart, J.-F. Colomer, T. Tabarrant, J.-P. Vigneron, New J. Phys. 10 (2008) 033014.

- [9] F. Liu, B.Q. Dong, X.H. Liu, Y.M. Zheng, J. Zi, *Opt. Exp.* 17 (2009) 16183-16191.
- [10] M. Rassart, P. Simonis, A. Bay, O. Deparis, J.-P. Vigneron, *Phys. Rev. E* 80 (2009) 031910.
- [11] J.H. Kim, J.H. Moon, S.-Y. Lee, J. Park, *Appl. Phys. Lett.* 97 (2010) 103701.
- [12] M.N. Ghazzal, O. Deparis, J. De Coninck, E.M. Gaigneaux, *J. Mater. Chem. C* 1 (2013) 6202-6209.
- [13] R.A. Potyrailo, R.R. Naik, *Ann. Rev. Mater. Res.* 43 (2013) 307-334.
- [14] O. Deparis, M.N. Ghazzal, P. Simonis, S.R. Mouchet, H. Kebaïli, J. De Coninck, E.M. Gaigneaux, J.-P. Vigneron, *Appl. Phys. Lett.* 104 (2014) 023704.
- [15] R.A. Potyrailo, R.K. Bonam, J.G. Hartley, T.A. Starkey, P. Vukusic, M. Vasudev, T. Bunning, R.R. Naik, Z. Tang, M.A. Palacios, M. Larsen, L.A. Le Tarte, J.C. Grande, S. Zhong, T. Deng, *Nat. Comm.* 6 (2015) 7959.
- [16] O. Poncelet, G. Tallier, S.R. Mouchet, A. Crahay, J. Rasson, R. Kotipalli, O. Deparis, L.A. Francis, *Bioinspir. Biomim.* 11 (2016) 036011.
- [17] M.R. Baklanov, K.P. Mogilnikov, V.G. Polovinkin, F.N. Dultsev, *J. Vac. Sci. Technol. B* 18 (2000) 1385-1391.
- [18] C.W. Mason, *J. Phys. Chem.* 27 (1923) 201-251.
- [19] C.W. Mason, *J. Phys. Chem.* 30 (1926) 383-395.
- [20] C.W. Mason, *J. Phys. Chem.* 31 (1927) 321-354.
- [21] C.W. Mason, *J. Phys. Chem.* 31 (1927) 1856-1872.
- [22] X. Yang, Z. Peng, H. Zuo, T. Shi, G. Liao, *Sensors Actuat. A* 167 (2011) 367-373.
- [23] X. Jiang, T. Shi, H. Zuo, X. Yang, W. Wu, G. Liao, *Sci. China Technol. Sci.* 55 (2012) 16-21.
- [24] W. Wang, W. Zhang, X. Fang, Y. Huang, Q. Liu, J. Gu, D. Zhang, *Sci. Rep.* 4 (2014) 5591.
- [25] P. Vukusic, J.R. Sambles, C.R. Lawrence, R.J. Wootton, *Proc. R. Soc. Lond. B* 266 (1999) 1403-1411.
- [26] S. Berthier, *Photonique des Morphos*, Springer, Paris, 2010.
- [27] P. Vukusic, I. Hooper, *Science* 310 (2005) 1151.
- [28] T.M. Trzeciak, B.D. Wilts, D.G. Stavenga, P. Vukusic, *Opt. Exp.* 20 (2012) 8877-8890.
- [29] H.E. Hinton, G.M. Jarman, *Nature* 238 (1972) 160-161.
- [30] S. Berthier, *Iridescences, les couleurs physiques des Insectes*, Springer, Paris, 2003.
- [31] J.-P. Vigneron, J.-F. Colomer, N. Vigneron, V. Lousse, *Phys. Rev. E* 72 (2005) 061904.
- [32] S.R. Mouchet, B.-L. Su, T. Tabarrant, S. Lucas, O. Deparis, *Proc. SPIE* 9127 (2014) 91270U.
- [33] O. Deparis, S.R. Mouchet, L. Dellieu, J.-F. Colomer, M. Sarrazin, *Mater. Today Proc.* 1S (2014) 122-129.
- [34] S.R. Mouchet, E. Van Hooijdonk, V.L. Welch, P. Louette, J.-F. Colomer, B.-L. Su, O. Deparis, *Sci. Rep.* 6 (2016) 19322.
- [35] R.A. Potyrailo, H. Ghiradella, A. Vertiatchikh, K. Dovidenko, J.R. Courmoyer, E. Olson, *Nat. Photonics* 1 (2007) 123-128.
- [36] Y. Gao, Q. Xia, G. Liao, T. Shi, T., *J. Bionic Eng.* 8 (2011) 323-334.
- [37] T. Jiang, Z. Peng, W. Wu, T. Shi, G. Liao, *Sensors Actuat. A* 213 (2014) 63-69.
- [38] R.A. Potyrailo, T. A. Starkey, P. Vukusic, H. Ghiradella, M. Vasudev, T. Bunning, R.R. Naik, Z. Tang, M. Larsen, T. Deng, S. Zhong, M. Palacios, J.C. Grande, G. Zorn, G. Goddard, S. Zalubovsky, *P. Natl. Acad. Sci. USA* 110 (2013) 15567-15572.
- [39] L.P. Biró, K. Kertész, Z. Vértésy, *Zs. Bálint, Proc. SPIE* 7057 (2008) 705706.
- [40] K. Kertész, G. Piszter, E. Jakab, *Zs. Bálint, Z. Vértésy, L.P. Biró, Appl. Surf. Sci.* 281 (2013) 49-53.
- [41] G. Piszter, K. Kertész, Z. Vértésy, *Zs. Bálint, L.P. Biró, Opt. Exp.* 22 (2014) 22649-22660.
- [42] K. Kertész, G. Piszter, E. Jakab, *Zs. Bálint, Z. Vértésy, L.P. Biró, Mater. Sci. Eng. C* 39 (2014) 221-226.
- [43] I. Tamáska, K. Kertész, Z. Vértésy, *Zs. Bálint, A. Kun, S.-H. Yen, L.P. Biró, J. Insect Sci.* 13 (2013) 1-15.
- [44] K. Kertész, G. Piszter, Z. Baji, E. Jakab, Z. Bálint, Z. Vértésy, *L.P. Biró, Chem. Sensors* 4 (2014) 17.
- [45] G. Piszter, K. Kertész, Z. Vértésy, *Zs. Bálint, L.P. Biró, Anal. Method.* 3 (2011) 78-83.
- [46] Z. Wang, J. Zhang, J. Xie, C. Li, Y. Li, S. Liang, Z. Tian, T. Wang, H. Zhang, H. Li, W. Xu, B. Yang, *Adv. Funct. Mater.* 20 (2010) 3784-3790.
- [47] L. Bai, Z. Xie, W. Wang, C. Yuan, Y. Zhao, Z. Mu, Q. Zhong, Z. Gu, *ACS Nano* 8 (2014) 11094-11100.
- [48] Y.Y. Diaó, X.Y. Liu, G.W. Toh, L. Shi, J. Zi, *Adv. Func. Mater.* 23 (2013) 5373-5380.
- [49] R.A. Potyrailo, C. Surman, N. Nagraj, A. Burns, *Chem. Rev.* 111 (2011) 7315-7354.
- [50] X. Liu, S. Cheng, H. Liu, S. Hu, D. Zhang, H. Ning, *Sensors* 12 (2012) 9635-9665.
- [51] F. Bernoux, J.-P. Piel, B. Castellon, C. Defranoux, J.-H. Lecat, P. Boher, J.-L. Stehlé, *Tech. Ing., tr. Mes. Contr.* R6490 (2003), 1-11.
- [52] S.J. Gregg, K.S.W. Sing, *Adsorption, Surface Area and Porosity*, Academic Press, second edition, Londres, 1982.
- [53] P.A. Webb, C. Orr, *Analytical Methods in Fine Particle Technology*, Micromeritics Instrument Corporation, Norcross, 1997.
- [54] O. Kadlec, M.M. Dubinin, *J. Colloid Interf. Sci.* 31 (1969) 479-489.
- [55] G.A. Andreeva, N.S. Polyakov, M.M. Dubinin, K.M. Nikolaev, *B. Acad. Sci. USSR Ch.* 30 (1982) 1795-1799.
- [56] S.R. Mouchet, O. Deparis, J.-P. Vigneron, *Proc. SPIE* 8424 (2012) 842425.
- [57] S.R. Mouchet, T. Tabarrant, S. Lucas, B.-L. Su, P. Vukusic, O. Deparis, *Opt. Exp.* 24 (2016) 12267-12280.
- [58] P. Yeh, *Optical Waves in Layered Media*, Wiley-Interscience, New York, 2005.
- [59] I.B.J. Sollas, *Proc. R. Soc. Lond. B* 79 (1907) 474-481.
- [60] H. Arwin, *Thin Solid Films* 519 (2011) 2589-2592.
- [61] H. Arwin, T. Berling, B. Johs, K. Järrendahl, *Opt. Exp.* 21 (2013) 22645-2656.
- [62] L. Fernández del Río, H. Arwin, K. Järrendahl, *Thin Solid Films* 571 (2014) 410-415.